CALCULATION OF THE PERFORMANCE OF SOLAR CELLS WITH SPECTRAL DOWN SHIFTERS USING REALISTIC OUTDOOR SOLAR SPECTRA

W.G.J.H.M. van Sark

Department of Science, Technology and Society, Copernicus Institute for Sustainable Development and Innovation,
Utrecht University, Heidelberglaan 2, 3584 CS Utrecht, the Netherlands,
T: +31 30 253 7611, F: +31 30 253 7601, E: w.g.j.h.m.vansark@uu.nl

ABSTRACT: Spectral down converters and shifters have been proposed as a good means to enhance the efficiency of underlying solar cells. In this paper, we focus on the simulation of the outdoor performance of solar cells with spectral down shifters, i.e., multicrystalline silicon solar cells with semiconductor nanocrystals as wavelength-shifting material. Daily and annual performance of these devices can be simulated using spectra that vary over the course of the day. However, as these spectra are not systematically measured, we have employed a spectrum simulation model that is able to simulate clear and also cloudy days: SEDES2. Through the availability of experimentally determined global, direct, and diffuse irradiation data on a minutely basis, we were able to model a full year of spectra for the Netherlands. These spectra are aggregated to yield hourly spectra, which are subsequently used in modelling the solar cell output. We have determined the performance of spectral converters for a number of typical days: a clear summer day, a cloudy summer day, a clear winter day, and a cloudy winter day. It was found that the simulated short current enhancement, which varies between about 7 and 23%, is linearly related with the average photon energy of the spectra. As this is also found to hold for monthly averaged spectra, we were able to calculate an annual performance increase of 12.8% for the present down shifting layer on top of multicrystalline solar cells in the Dutch climate.
Keywords: Modelling; Solar cell; Energy performance, Average photon energy, Down shifting

1 INTRODUCTION

One of the many possible ways to improve the performance of solar cells is to attain a better matching of the incident spectrum with the spectral response of the solar cell. This may be possible by modification of the out- or indoor spectrum by means of down and/or up conversion, and down shifting. In case of down conversion an incident high-energy photon is converted into two or more lower energy photons; for up-conversion two or more low energy photons (sub band gap) are converted into one high-energy photon. Down shifting is similar to down conversion albeit that the quantum efficiency of the conversion process is unity, while that of shifting is lower than unity [1], but preferable as close as possible to unity.

Several modelling studies on incorporation of conversion layers on top (down converter or shifter) or at the bottom (up converter) of single junction solar cells have shown that the conversion efficiency may increase by about 10% [2-7]. Experimental work has shown a 6-% relative increase in conversion efficiency for coating a multi-crystalline silicon solar cell with a downshifting layer [8]. Coating of a CdS/CdTe solar cell with a layer that contained a fluorescent colouring agent was reported to lead to an increase of the spectral response in the blue, while a maximum increase in efficiency was calculated to be 30-40% [9].

Previously, we have modelled performance enhancement of solar cells resulting from inclusion of semiconductor nanocrystals or quantum dots (QDs) in a plastic layer on top of solar cells. Such layers may be denoted as down shifters (DSs). Modelling results showed a 10% increase in short circuit current under AM1.5 [6]. These results were based on existing designs of multicrystalline silicon solar cells, and the spectral down shifter properties (QD concentration and size) were optimized. Past, present and future cell designs have been compared [10], and it was shown that the improved cell designs were modelled to have a lower efficiency benefit from DS application than the older cell design: for the AM1.5G spectrum the current increase was 10, 8.5, and 7.5%, for the past, present, future cell design, respectively.

The efficiency of solar cells depends mainly on two irradiance properties, i.e., the irradiation intensity [11] and the spectral composition of incident light [12]. Both intensity and spectral composition vary depending on time (seasonal and daily variation), geographical location, presence of clouds, and air pollution. Estimation of the annual performance of solar cells thus requires actual or typical irradiation distributions as input, e.g., for a particular location [13]. The short circuit current increase for DSs on top of solar cells for non-AM1.5 clear sky spectra has been modelled to be larger (up to 30%) than for AM1.5 conditions [7]. As actually occurring spectra also include cloudy conditions, with expected blue-shifted spectra compared compare to AM1.5, it is expected that an increase in annual performance of such devices may be between 10 and 30%.

In this paper the performance of solar cells with DSs is estimated under realistic irradiation conditions, i.e., for varying spectral distributions as they may be found outdoors. The spectral distributions that we used for this evaluation were generated on a minutely basis by means of the spectrum simulation model SEDES2 [14]. Inputs for the model were minutely data for global, direct, and diffuse irradiation as well as other measured weather data from a meteorological measuring station in the Netherlands. The minutely spectra generated by the SEDES2 model were subsequently aggregated to yield hourly spectra, which are then used in modelling the output of the solar cell with and without DS. In this paper we will demonstrate the performance enhancement due to DSs for a number of typical days: a clear summer day, a cloudy summer day, a clear winter day, and a cloudy winter day. From the found relation between performance enhancement and average photon energy of the spectra, and using monthly aggregated spectra the annual performance enhancement can be calculated.

2 METHODOLOGY

Two independent models were employed in this study. First, the SEDES2 spectral model was utilized to generate minutely spectral data. These spectra were aggregated to hourly and monthly data; also four typical days were selected. These spectra were applied in the calculation of solar cell performance using PC1D [15]. Results are compared for solar cells with and without spectral down shifter.

2.1 Spectral data simulation

Measured solar spectral data are not available in most countries, as also is the case for the Netherlands, due to the lack of spectral measurement stations. Therefore we modelled the spectra by employing the SEDES2 spectral model [14]. SEDES2 is an extension of SPCTRAL2 [16] that is able to model clear-sky spectra. SEDES2 includes modelling of spectra for cloudy skies, and was updated recently [17]. Required model inputs are total, diffuse and direct irradiance, ambient temperature, site's pressure, and relative humidity, on any time base. The spectra are calculated in the wavelength range of 300-1400 nm.

Since March 2005, the Royal Netherlands Meteorological Institute (KNMI) has established its own irradiance measurement station, which continuously records the total, diffuse, and direct irradiance every minute at geographical location of 51.971ºN, 4.927ºE in Cabauw, a location close to the city of Utrecht. It is part of the Baseline Surface Radiation Network (BSRN) (http://bsrn.ethz.ch/). The data are used in order to derive minutely simulated solar spectrum for a one-year period from March 1st 2005 to February 28th 2006, constituting a full year. Ambient temperature, relative humidity, and pressure were measured on site near (< 100 m) to the irradiance measurement set-up. Spectra are calculated by SEDES2 for a 37° tilted surface directed towards the south. We thus can compare the spectra with the ASTM AM1.5G standard [18]. More details are given in [19], in which also the spectral effects on amorphous and crystalline silicon solar cells are discussed.

2.2 Solar cell configuration and simulation

The configuration studied is a highly transparent layer containing QDs on top of a solar cell (Fig. 1) [6]. Generally, the size of the QDs is taken such that both blue and green light is absorbed and emitted in the red, which corresponds to an optimum spectral response of the solar cell. Depending on the QD concentration also unabsorbed blue and green light enters the solar cell.

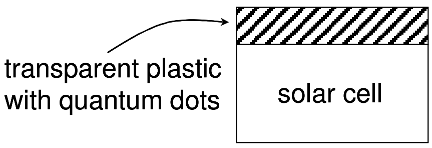

Figure 1: Schematic drawing of the studied configuration. A plastic layer containing QDs is applied on top of a solar cell. Absorption of incident light and emission lead to a modified spectrum incident on the solar cell.

For solar cell simulation we use material and device parameters (status 2005 [20]) for the standard 12.5×12.5 cm^2 baseline n-p-p^+ mc-Si cell developed at the Energy research Centre of the Netherlands (ECN), which has parameters that are typical of low-cost commercial cells, including series resistance, shunt conductance and a second diode. The cell thickness is 300 µm, the cell has a shallow diffused emitter, and the 9 µm thick back-surface-field (BSF) has a p^+ surface doping level of 4×10^{18} cm^{-3}. The front surface anti-reflection coating consists of 71-nm thick silicon nitride with a refractive index n=2.1 deposited by means of an in-line Microwave Remote Plasma CVD process [21]. The performance of the solar cell is simulated with the simulation programme PC1D (version 5.8) [15], using incident spectra that are modified by the downshifting layer. The cell parameters without down shifter are: open circuit voltage 0.624 V, short circuit current 35.4 mA/cm^2, fill factor 0.773, efficiency 17.1 %.

2.3 Spectrum modification

The incident spectrum, i.e. the amount of photons per wavelength $\Phi_s(\lambda)$, is modified by absorption of photons in the downshifting layer. The amount of absorbed photons in this layer $\Phi_a(\lambda)$ is determined from the QD absorption spectrum, which depends on the QD size, their concentration in the downshifting layer, and the thickness of this layer. This absorbed amount is subtracted from the incident spectrum: $\Phi_{sa}(\lambda) = \Phi_s(\lambda) - \Phi_a(\lambda)$. As the QDs re-emit light at a red-shifted wavelength, the amount of emitted photons $\Phi_e(\lambda)$ is calculated from the QD emission spectrum. To this end, a quantum efficiency (QE) of 0.8 [22] is assumed, as well as the assumption that ¾ of the emitted photons is directed towards the underlying solar cell, due to internal reflection in the converter layer [23]. The amount of emitted photons is then added to the already modified spectrum: $\Phi_{sae}(\lambda) = \Phi_s(\lambda) - \Phi_a(\lambda) + \Phi_e(\lambda)$, and the resulting spectrum serves as input for the solar cell simulation model.

Absorption of photons is calculated by using the Lambert-Beer equation: the photon flux density $\Phi(x,\lambda)$ after passing a distance x in a film with absorption coefficient $\alpha(\lambda)$ is written as $\Phi(x,\lambda) = \Phi^0(\lambda)\ exp[-\alpha(\lambda)x]$, with $\Phi^0(\lambda)$ the incident photon flux density. The exponential term $\alpha(\lambda)x$ equals $\varepsilon_\lambda CD$, with ε_λ the molar extinction coefficient ($M^{-1}cm^{-1}$), C the chromophore concentration (M), and D the thickness of the film (cm). The molar extinction coefficient is determined by scaling the normalized absorption spectrum such that the molar extinction coefficient ε_λ at 350 nm equals $\varepsilon_\lambda=1.438\times10^{26}\,a^3$ [24]. The QD radius a is determined from the absorption maximum and the known relation with particle diameter [25]. The QD concentration can be easily varied, and earlier studies have revealed an option concentration of 100 µM, for a QD emitting at 603 nm and a down shifter thickness of D of 0.1 cm [6].

3 RESULTS AND DISCUSSION

3.1 Spectral data simulation

From over 200,000 spectra that were modelled at first four typical days were selected, representing the occurring extremes of variation in spectral composition in irradiation conditions during one year in the Netherlands: a clear summer day (19 June), a cloudy summer day, 3 June), a clear winter day (25 December), and a cloudy winter day (11 December) [19]. Figures 2 and 3 respectively show the irradiation intensity as a function of time for these four days and their spectra as a function of time. These hourly spectra are constructed from 60 minutely spectra. The modelled spectra for the summer days are similar to the ASTM AM1.5 standard, as can be inferred from Fig. 3.

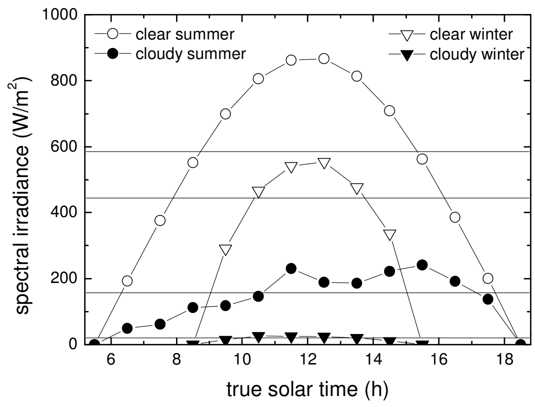

Figure 2: Spectral irradiance variation as a function of true solar time for the four days as shown in Fig.3. Average irradiances are indicated by the solid lines

Monthly aggregated spectra were constructed from the minutely spectra for all available 12 months. The monthly global irradiances are depicted in Fig. 4, together with the annual average spectrum. The monthly sums are shown in Fig. 5; the annual sum for these months is 1076.4 kWh/m^2.

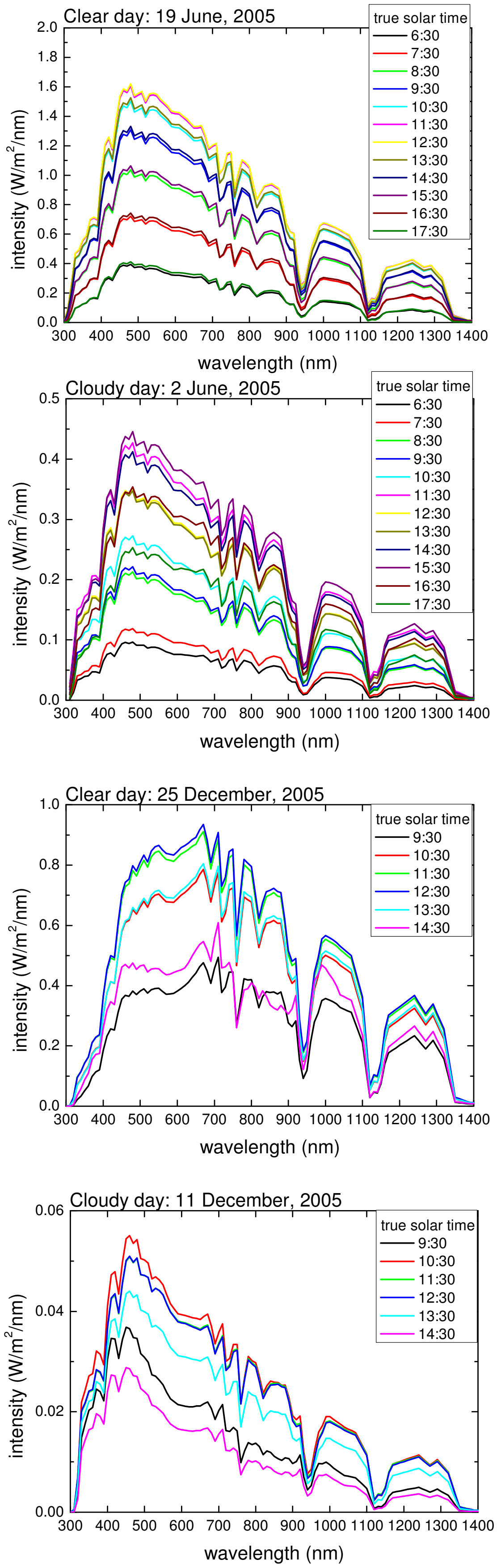

Figure 3: Hourly spectra aggregated from calculated minutely spectra using SEDES2 and measured irradiation and meteorological data for four days: clear summer day (19 June); cloudy summer day (11 June); clear winter day (25 December); cloudy winter day (11 December). Hours are given in true solar time

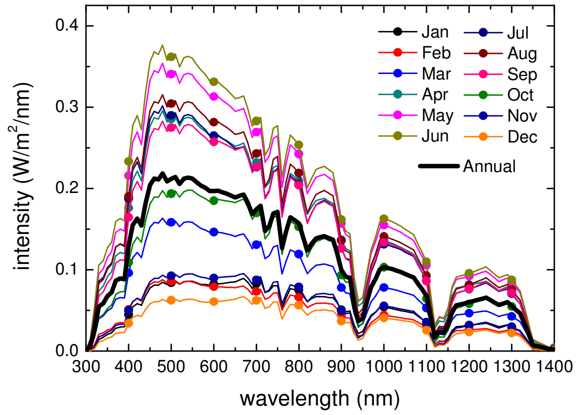

Figure 4: Monthly spectra and the annual spectrum aggregated from calculated minutely spectra using SEDES2 and measured irradiation and meteorological data

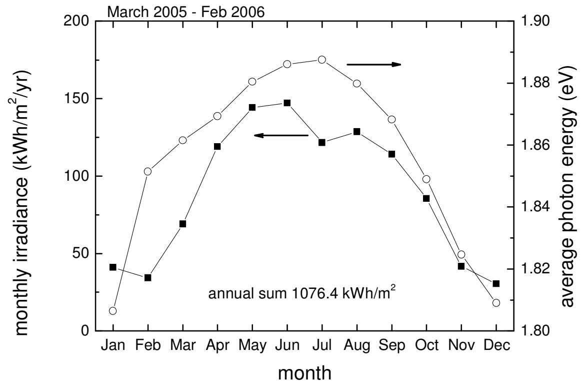

Figure 5: Monthly irradiance sums and average photon energy for the 12 months

The weighted average photon energy (APE), calculated for the 350-1050 nm range as used by Minemoto *et al.* [26], can be used as being characteristic of the spectrum. This wavelength range is particularly useful for crystalline silicon. The APE varies between 1.878 and 1.920, for the modelled clear and cloudy summer days, which is slightly higher than the 1.875 eV APE value that is found for the AM1.5 standard spectrum. The APEs of the clear winter day are smaller than the AM1.5 value and vary between 1.748 and 1.785 eV, while the APEs of the cloudy winter day are larger and vary between 1.935 and 2.025 eV. The daily average spectral irradiances for the summer days are 585 W/m^2 (clear) and 157 W/m^2 (cloudy); for the winter days they are 444 W/m^2 (clear) and 20.4 W/m^2 (cloudy), as indicated in Fig. 2. The APEs for the 12 months are also shown in Fig. 5. The annual APE is 1.868 eV, which is slightly smaller than the APE of the AM1.5 standard spectrum. Note the apparent relation between monthly irradiance sums and APE.

3.2 Solar cell simulation

Earlier work has revealed that the optimum QD concentration is 100 µM for a downshifter thickness of 1 mm and QDs emitting at 603 nm, for both AM1.5 and non-AM1.5 spectra [6, 7], and also for different solar cell material quality [10]. We therefore used these data to calculate the cell's performance parameters.

Figure 6 shows the simulated short circuit current as a function of true solar time for the four typical days

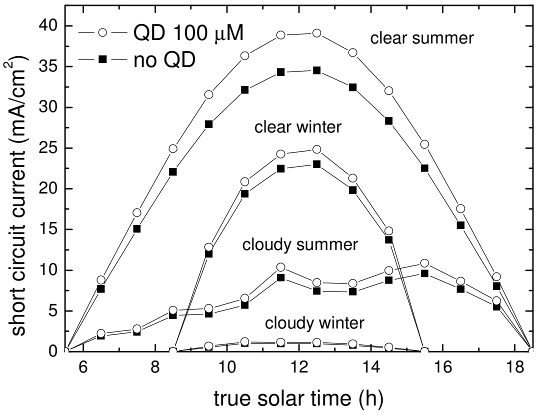

Figure 6: Short circuit current increase for the used solar cell with a down shifting layer with and without QDs calculated for the four typical summer and winter days. QD concentration is 100 µM, and emit at 603 nm. Down shifter thickness is 1 mm

Table I: Average photon energy (350-1050 nm) and short circuit current increase, with standard deviation of their means, for the four typical days

day	APE (eV)	J_{sc} increase (%)
clear summer day	1.895	13.2 ± 0.4
cloudy summer day	1.897	13.7 ± 0.6
clear winter day	1.774	7.7 ± 0.4
cloudy winter day	1.962	17.9 ± 2.9

comparing the down shifter without and with QDs. It is clear that the short circuit current is enhanced for all cases. The maximum current increase is 22.9% for the cloudy winter day at 14:30h; the minimum current increase is 6.9% for the clear winter day at 8:30h. Daily averages are shown in Table I, and are compared with the APE. From the standard deviations in the mean for all but the cloudy winter day it is inferred that both APE and the short circuit current increase are not varying much over the course of the day.

Interestingly, the data in this table suggest a possible relation between average short circuit increase and APE; we therefore have plotted the relative short circuit current $J_{sc,rel}$ as a function of APE in Fig. 7. The data can well be fitted (R^2=0.986) by means of the linear equation

$$J_{sc,rel} = a + b \times APE \qquad (1)$$

and we find $a = 0.12 \pm 0.03$ and $b = 0.535 \pm 0.015$.

This apparent linear relationship is further validated by calculating the short current increase for a number of other days, which have a varying clear sky index, see Fig. 8. In the same figure, the short circuit increase for the monthly spectra is shown to follow the linear relationship. The short circuit increase is found to vary between 9% and 13 % for the months January and July, respectively.

3.3 Annual performance enhancement

The linear relationship between the short circuit current increase and APE can be used to determine the annual current enhancement. To this end, we first show the annual distribution of APE in Fig. 9, calculated from 3615 hourly spectra with a bin size of 0.01 eV. From this figure we infer that 56% of the APE values are larger than the AM1.5 APE value. The annual current enhancement can now simply be calculated by multiplying the APE distribution with the linear

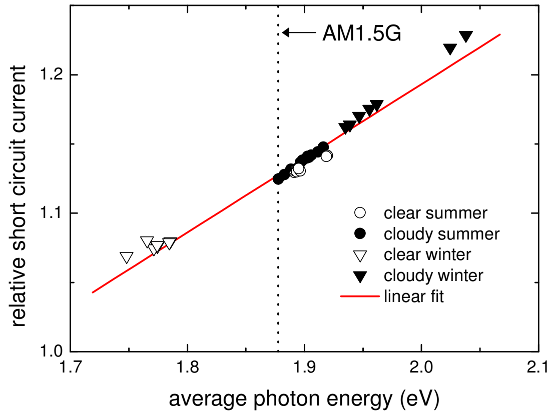

Figure 7: Relative short circuit current increase as a function of average photon energy for the four typical days

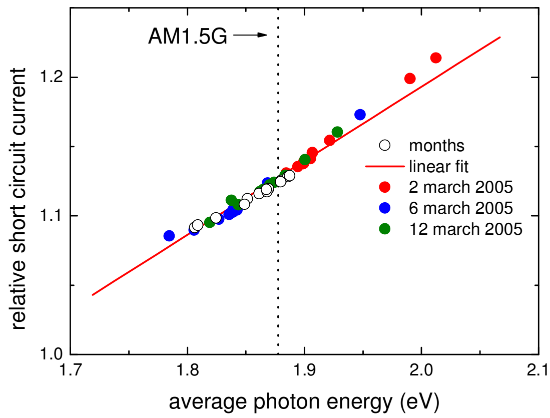

Figure 8: Relative short circuit current increase as a function of average photon energy for three other days and the 12 months

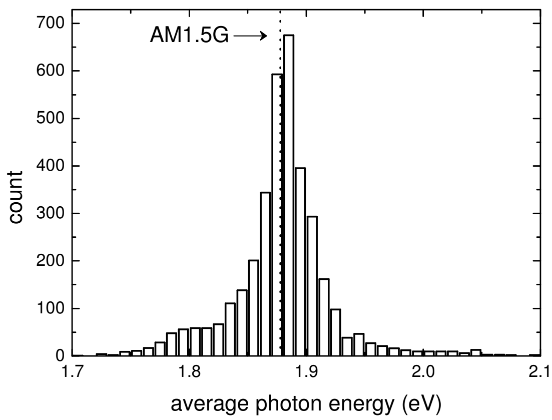

Figure 9: Distribution of average photon energy values calculated from hourly spectra

current enhancement that we found existed. We thus find that on an annual basis the current can be enhanced with 12.8%. Alternatively, we can use the annually averaged spectrum, as was shown in Fig. 4. The APE of this spectrum is 1.868 eV, and from Eq. (1) with constants a and b we calculate a current enhancement of 12.3%, which is about equal to the value we found before. The small difference is probably due to aggregation of the minutely spectra to hourly ones before the APE is calculated.

Note that the simulations do not take into account that the angle of incidence of irradiation varies over the course of the day; instead only normal incidence is studied. Non-normal incidence would increase absorption in the down shifter, leading to a somewhat larger emission at the emission wavelength, and consequently to a somewhat larger current increase. The simulations presented here thus reveal a conservative estimate of the current increase possibly to be attained including down shifters on top of solar cells.

4 CONCLUSIONS

The annual performance enhancement in terms of short circuit increase of solar cells with a down shifter on their topside has been investigated using modelled spectra. A relation has been found between the short circuit current increase and the average photon energy of a spectrum from considering hourly spectra of four typical and other randomly selected days throughout the year, and of monthly spectra. A maximum short circuit increase of 22.9% is found for a cloudy winter day, corresponding to a high average photon energy value. A minimum short circuit increase of 6.9% is found for a clear winter day, corresponding to a low average photon energy value. The short circuit increase on a monthly basis varies between 9% and 13% for the months January and July, respectively. The annual short circuit increase is determined using the annual distribution of APE values and their linear relation: it is calculated to be 12.8%

5 ACKNOWLEDGEMENTS

We gratefully acknowledge Bamshad Houshyani Hassanzadeh (UU) for extensive spectral modelling, Daryl Myers (National Renewable Energy Laboratory, NREL, USA) for enthusiastically updating SEDES2, Wouter Knap and Alexander Los (KNMI) for supplying Dutch irradiation data, Cees Tool and Arthur Weeber (Energy research Centre of the Netherlands (ECN)) for supplying cell design parameters, Nils Reich and Erik Alsema (UU) for critical reading of the manuscript, and the European Commission for financial support as part of the Framework 6 integrated project FULLSPECTRUM (contract SES6-CT-2003-502620).

6 REFERENCES

[1] B.S. Richards, Solar Energy Materials and Solar Cells 90 (2006) 2329.
[2] B.S. Richards, Solar Energy Materials and Solar Cells 90 (2006) 1189.
[3] T. Trupke, A. Shalav, B.S. Richards, P. Wurfel, M.A. Green, Solar Energy Materials and Solar Cells 90 (2006) 3327.
[4] C. Strumpel, M. McCann, G. Beaucarne, V. Arkhipov, A. Slaoui, V. Svrcek, C. del Canizo, I. Tobias, Solar Energy Materials and Solar Cells 91 (2007) 238.
[5] G.C. Glaeser, U. Rau, Thin Solid Films 515 (2007) 5964.
[6] W.G.J.H.M. Van Sark, A. Meijerink, R.E.I. Schropp, J.A.M. Van Roosmalen, E.H. Lysen, Solar Energy Materials and Solar Cells 87 (2005) 395.
[7] W.G.J.H.M. Van Sark, Applied Physics Letters 87 (2005) 151117.
[8] T. Maruyama, J. Bandai, Journal of the Electrochemical Society 146 (1999) 4406.
[9] T. Maruyama, R. Kitamura, Solar Energy Materials and Solar Cells 69 (2001) 61.
[10] W.G.J.H.M. Van Sark, Proceedings of the 21st European Photovoltaic Solar Energy Conference (2006) 155.
[11] N.H. Reich, W.G.J.H.M. Van Sark, E.A. Alsema, S.Y. Kan, S. Silvester, A.S.H. Van der Heide, R.W. Lof, R.E.I. Schropp, Proceedings 20th European Photovoltaic Solar Energy Conference (2005) 2120.
[12] S. Nann, K. Emery, Solar Energy Materials and Solar Cells 27 (1992) 189.
[13] W.G.J.H.M. Van Sark, European Journal of Physics 28 (2007) 415.
[14] S. Nann, C. Riordan, Journal of Applied Meteorology 30 (1991) 447.
[15] P.A. Basore, D.A. Clugston, Proceedings 25th IEEE Photovoltaic Specialists Conference (1996).
[16] R.E. Bird, C. Riordan, Journal of Climate and Applied Meteorology 25 (1986) 87.
[17] Personal communication D.R. Myers (2006).
[18] ASTM, Standard Tables for Reference Solar Spectral Irradiances: Direct Normal and Hemispherical on 37° Tilted Surface, Standard G173-03e1 2003, West Conshohocken, PA, USA.
[19] B. Houshyani Hassanzadeh, A.C. de Keizer, N.H. Reich, W.G.J.H.M. van Sark, this conference.
[20] C.J.J. Tool, G. Coletti, F.J. Granek, J. Hoornstra, M. Koppes, E.J. Kossen, H.C. Rieffe, I.G. Romijn, A.W. Weeber, Proceedings 20th European Photovoltaic Solar Energy Conference (2005) 578.
[21] W. Soppe, H. Rieffe, A. Weeber, Progress in Photovoltaics: Research and Applications 13 (2005) 551.
[22] L. Qu, X. Peng, Journal of the American Chemical Society 124 (2002) 2049.
[23] A.J. Chatten, K.W.J. Barnham, B.F. Buxton, N.J. Ekins-Daukes, M.A. Malik, Proceedings Third World Congress on Photovoltaic Energy Conversion (WPEC-3) (2003) 2657.
[24] C.A. Leatherdale, W.-K. Woo, F.V. Mikulec, M.G. Bawendi, Journal of Physical Chemistry B 106 (2002) 7619.
[25] B.O. Dabbousi, J. Rodriguez-Viejo, F.V. Mikulec, J.R. Heine, H. Mattoussi, R. Ober, K.F. Jensen, M.G. Bawendi, Journal of Physical Chemistry B 101 (1997) 9463.
[27] T. Minemoto, M. Toda, S. Nagae, M. Gotoh, A. Nakajima, K. Yamamoto, H. Takakura, Y. Hamakawa, Solar Energy Materials and Solar Cells 91 (2007) 120.